Three-element matching networks for receive-only MRI coil decoupling

Wang, Wenjun; Zhurbenko, Vitaliy; Sánchez-Heredia, Juan Diego; Ardenkjær-Larsen, Jan Henrik

Published in:
Magnetic Resonance in Medicine

Link to article, DOI:
10.1002/mrm.28416

Publication date:
2021

Document Version
Peer reviewed version

Received: 27 March 2020 | Revised: 15 June 2020 | Accepted: 16 June 2020

DOI: 10.1002/mrm.28416

NOTE

Magnetic Resonance in Medicine

Three-element matching networks for receive-only MRI coil decoupling

Wenjun Wang | **Vitaliy Zhurbenko** | **Juan Diego Sánchez-Heredia** | **Jan Henrik Ardenkjær-Larsen**

Department of Electrical Engineering, Technical University of Denmark (DTU), Kongens Lyngby, Denmark

Correspondence
Vitaliy Zhurbenko, Department of Electrical Engineering, Technical University of Denmark (DTU), Kongens Lyngby 2800, Denmark.
Email: vz@elektro.dtu.dk

Funding information
Danmarks Grundforskningsfond, Grant/Award Number: DNRF 124

Purpose: Preamplifier decoupling is useful for minimizing interaction between MRI array elements. The purpose of this work is to propose a general approach to designing networks for preamplifier decoupling while keeping the number of elements to a minimum. The approach is applicable to arbitrary impedance preamplifiers and arbitrary coil impedances.

Methods: Closed form design equations for decoupling networks are derived based on maximum decoupling and minimum preamplifier noise conditions. The analytical solutions are verified using numerical simulations. Design examples at 32.1, 64, 128, and 298 MHz are shown. One of the examples is realized on a test bench. The fabricated circuit is tested for decoupling and minimum noise properties.

Results: The design equations are verified numerically and experimentally. The fabricated network demonstrates 30.7 dB of decoupling and minimum output noise at the design frequency.

Conclusion: The design equations lead to four alternative network solutions. Each network is realized as a T-shape or Π-shape three elements circuit topology. All four networks are identical in performance providing minimum amplifier noise and maximum decoupling for a given preamplifier and coil combination. An MRI array designer can choose any solution out of four. The considerations for choosing the most practical solution are given. The presented method enables the use of arbitrary impedance preamplifiers or transistors (not necessary 50 Ω) and provides the most compact design possible (with the least number of components), which is particularly useful in multi-element systems.

KEYWORDS
impedance matching, MRI array, optimal noise matching, preamplifier decoupling

1 | INTRODUCTION

The detectors in the MRI systems are often arranged into arrays, and the spatial proximity of detector coils leads to mutual coupling and detuning. This greatly complicates the impedance matching procedure. It has been shown that it is possible to maximize combined SNR in the presence of mutual coupling.[1] Notwithstanding, suppressing mutual

coupling is generally considered a more convenient approach. Suppression of mutual coupling is possible by careful spatial arrangement of array elements.[2] Yet, preamplifier decoupling, where array elements are nearly open circuited,[2-4] allows for more flexibility in spatial element arrangement.

Matching networks providing a large impedance at the terminals of the coil are used in preamplifier decoupling. At the same time, these networks transform the coil impedance to the optimal noise impedance of the preamplifier[5] to minimize noise coming from the active element (transistor). There have been several design methods for such networks. For example, Johansen et al[6] showed a general approach to network design with several steps of impedance transformation involving transmission lines. The approach[6] can be used to design a five-element matching network, although reduction in number of elements is possible. Reykowski et al[7] showed the design of a four-element matching network that presents flexibility in the choice of element values. The design approach relies on preamplifiers with purely real optimal noise impedance (typically 50 Ω), although one can easily extend it to complex impedances with additional circuit components.

As will be shown in this paper, a minimum of three circuit elements is required to construct such a noise matching and decoupling network for an arbitrary impedance coil and an arbitrary optimal noise impedance preamplifier. A general approach to designing all possible topologies of such three-element networks is developed in this work. The design equations presented here are derived using the same matching and decoupling conditions as in the methods outlined above,[2,6,7] and therefore leads to the same decoupling level and minimum noise conditions. Because the described networks are capable of matching complex impedance coils to complex optimal noise impedance preamplifiers, this approach increases design flexibility. The approach enables use of a wider variety of preamplifiers and transistors, which do not have to be pre-matched to the system impedance, for example, 50 Ω, and therefore, might have wider bandwidths, better noise, and decoupling performance. Relying on a minimum number of circuit elements—three in this case—might also lead to a compact design, which is useful in constructing dense MRI arrays. Approaches with a larger number of circuit elements, for example, four-element network described by Reykowski et al,[7] allow for flexibility with regard to the choice of the component values. The three-element design approach described in this work offers four alternative solutions to choose from, still offering a reasonable degree of flexibility. To our knowledge, the design equations for all possible topologies of three-element decoupling networks for arbitrary coils and preamplifier noise impedances are presented here for the first time.

In the following sections, circuit topologies and corresponding design equations for three-element matching and decoupling networks are presented. The design flow is illustrated by a design example, where the circuit is also fabricated and tested.

2 | METHODS

In the outlined context, the purpose of the matching and decoupling circuit between the coil and the preamplifier, as shown in Figure 1, is (C1) to maximize coil decoupling, and (C2) to minimize preamplifier noise at the same time. Condition (C1) requires that the coil terminals should be presented with an impedance considerably larger than the impedance of the coil itself, ideally, infinitely large: $Z_{\text{in}} = \infty$ or $Y_{\text{in}} = 0$. The condition $Z_{\text{in}} = \infty$ inevitably imposes limitations on the input impedance of the preamplifier Z_a, as the circuit theory suggests[8]: if this impedance is finite, it must be purely reactive, that is, $Z_a = \mathrm{j}X_a$ or $Y_a = \mathrm{j}B_a$. Z_a is an inherent property of the implemented preamplifier. Obviously, such amplifiers and transistors do not exist in real world. Even though the real part of the input impedance of the preamplifier Z_a is in practice often smaller than the imaginary part, that is, $\Re\left(Z_a\right) \ll \left|\Im\left(Z_a\right)\right|$ or $\Re\left(Y_a\right) \ll \left|\Im\left(Y_a\right)\right|$, it is never

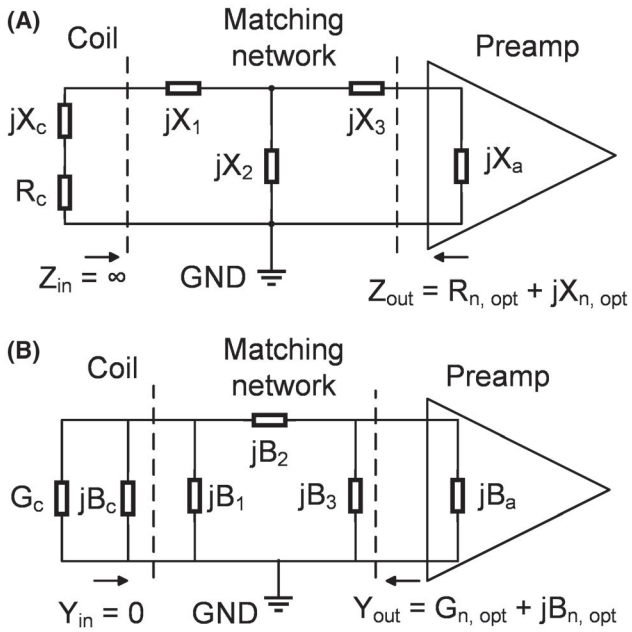

FIGURE 1 A, The T-matching network topology. B, The Π-matching network topology. The MRI coil is equivalently represented by a complex impedance $Z_c = R_c + \mathrm{j}X_c$ or admittance $Y_c = 1/Z_c = G_c + \mathrm{j}B_c$, where the real part describes the loss, and the imaginary part describes the coil reactance. The preamplifier has a complex optimal noise impedance, that is, $Z_{n,\text{opt}} = R_{n,\text{opt}} + \mathrm{j}X_{n,\text{opt}}$. For coil decoupling $Z_{\text{in}} = \infty$ or $Y_{\text{in}} = 0$ should be presented to the coil terminals. To minimise preamplifier noise $Z_{\text{out}} = Z_{n,\text{opt}}$ or $Y_{\text{out}} = Y_{n,\text{opt}}$ should be presented to the preamplifier input

zero. The consequence is that Z_{in} never reaches infinity but is a finite number in practice. Yet it satisfies condition (C1) for a given preamplifier.

Condition (C2) requires that the impedance of the coil transformed through the matching network Z_{out} is equal to the optimal noise impedance of the preamplifier $Z_{n,opt}$, and is expressed mathematically as $Z_{out} = Z_{n,opt}$. These conditions are illustrated in Figure 1, where the equivalent circuit models of the setup are shown.

The conditions (C1) and (C2) can be met using a circuit with at least three degrees of freedom, that is, three-element networks. For a three-element network, only T- and Π-topologies are possible.

In the following analysis, the MRI coil is represented by a complex impedance $Z_c = R_c + jX_c$ or admittance $Y_c = 1/Z_c = G_c + jB_c$, where the real part describes the loss, and the imaginary part describes the coil reactance. The preamplifier has a complex optimal noise impedance $Z_{n,opt} = R_{n,opt} + jX_{n,opt}$ or admittance $Y_{n,opt} = 1/Z_{n,opt} = G_{n,opt} + jB_{n,opt}$.

For the T-matching network topology (referred to as T-network hereafter) shown in Figure Figure 1A, the conditions (C1) and (C2) translate into system of three equations: $Z_{in} = \infty$, $\Re\left(Z_{out}\right) = R_{n,opt}$, and $\Im\left(Z_{out}\right) = X_{n,opt}$, which can be satisfied using a circuit with at least three degrees of freedom. Assuming the reactance of the components are X_1, X_2, and X_3, they should satisfy the system of the following equations:

$$\begin{cases} \left[\frac{1}{j(X_3+X_a)} + \frac{1}{jX_2}\right]^{-1} + jX_1 = \infty, \\ \left(\frac{1}{R_c+jX_c+jX_1} + \frac{1}{jX_2}\right)^{-1} + jX_3 = R_{n,opt} + jX_{n,opt}. \end{cases} \quad (1)$$

The solution of Equation 1 leads to

$$\begin{cases} X_2 = \pm\sqrt{R_c R_{n,opt}\left(1 + \frac{X_a'^2}{R_{n,opt}^2}\right)}, \\ X_3 = -X_a - X_2, \\ X_1 = -X_c \pm \sqrt{R_c R_{n,opt} - R_c^2 + \frac{R_c}{R_{n,opt}}\left(X_a' + X_2\right)^2}. \end{cases} \quad (2)$$

where $X_a' = X_a + X_{n,opt}$. The derivation of Equation 2 is given in the Supporting Information to this paper. The sign of X_2 can be either positive or negative, each corresponding to a set of solutions. However, the sign of X_1 is not related to the sign of X_2 and can be verified by substituting into Equation 1. Although Equation 2 is derived using relationship $Z_{in} = \infty$, Equation 2 is still valid for amplifiers with nonzero real input resistance, as discussed earlier.

For the Π-matching network topology (referred to as Π-network hereafter) shown in Figure 1B, the requirements are $Y_{in} = 0$, and $Y_{out} = Y_{n,opt} = G_{n,opt} + jB_{n,opt}$. Assuming the susceptances of the components are B_1, B_2, and B_3, the equations are:

$$\begin{cases} \left[\frac{1}{j(B_3+B_a)} + \frac{1}{jB_2}\right]^{-1} + jB_1 = 0, \\ \left(\frac{1}{G_c+jB_c+jB_1} + \frac{1}{jB_2}\right)^{-1} + jB_3 = G_{n,opt} + jB_{n,opt}. \end{cases} \quad (3)$$

The solution of Equation 3 leads to:

$$\begin{cases} B_2 = \pm\sqrt{G_c G_{n,opt}\left[1 + \left(\frac{B_c B_a' + G_{n,opt} G_c}{B_c G_{n,opt} - B_a' G_c}\right)^2\right]}, \\ B_3 = -B_2 - B_a - G_c \times \frac{B_a'^2 + G_{n,opt}^2}{B_c G_{n,opt} - B_a' G_c}, \\ B_1 = -B_2 - B_c - G_c \times \frac{B_c B_a' + G_{n,opt} G_c}{B_c G_{n,opt} - B_a' G_c}, \end{cases} \quad (4)$$

where $B_a' = B_a + B_{n,opt}$. The sign of B_2 can be either chosen positive or negative. Each sign corresponds to a solution set. Detailed derivation is given in the Supporting Information.

Four matching and decoupling networks can be designed for a given coil and preamplifier using Equations 2 and 4. The designer can choose any network among four for realization.

To demonstrate the method and outline the design flow, a simple surface loop coil described by Sánchez-Heredia et al[9] is used. The design frequency is 32.1 MHz, the resonance frequency of ^{13}C in a 3T static magnetic field. One of the solutions is realized on a test bench, and maximum decoupling and minimum preamplifier noise are verified experimentally. To demonstrate the applicability of the method to wider range of applications, examples at 64, 128, and 298 MHz are given at the end of the following section.

3 | RESULTS

This section presents the results of the design example developed using the theory described in the previous section. The measured impedance of the implemented coil loaded with a phantom is $Z_c = 0.11 + j11.7\,\Omega$, which corresponds to admittance $Y_c = 0.79 - j85.4\,mS$. The parameters of the preamplifier are usually provided by the manufacturer, and in this case, are extracted from the available preamplifier model.[10] The implemented preamplifier elcry1-u[10] has input impedance $Z_a = 109 - j863\,\Omega$, and the optimal noise impedance $Z_{n,opt} = 120 + j25.8\,\Omega$. The corresponding input admittance and optimal noise admittance of the preamplifier are $Y_a = 0.14 + j1.1\,mS$, and $Y_{n,opt} = 8.0 - j1.7\,mS$. Out of four possible solutions, a Π-network is realized here. The component values are calculated using Equation 4 (please refer to Figure 1B for topology and Figure Figure 2B for actual circuit realization):

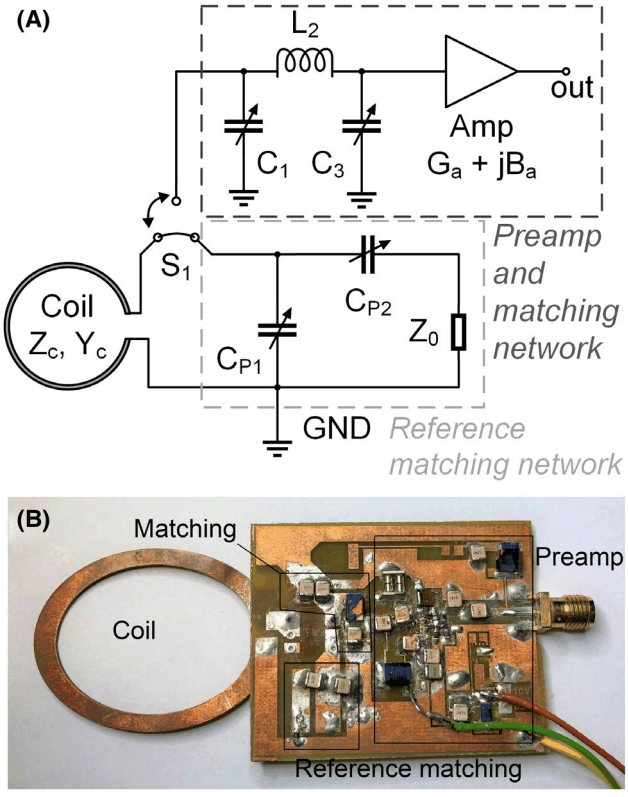

FIGURE 2 A, The circuit diagram of the fabricated matching network and the preamplifier. B, The photo of the fabricated circuit. On the PCB, there is a reference matching network and a preamplifier network. The coil can be connected to either the reference matching network or the preamplifier network to evaluate decoupling level

$$\begin{aligned} B_1 &= +88\,\text{mS} \Leftrightarrow C_1 = 440\,\text{pF}, \\ B_2 &= -2.5\,\text{mS} \Leftrightarrow L_2 = 2.0\,\mu H, \\ B_3 &= +1.4\,\text{mS} \Leftrightarrow C_3 = 7.2\,\text{pF}. \end{aligned} \tag{5}$$

These calculated values were verified numerically in Advanced Design System (ADS) software simulating circuit in Figure 2A.

First, G_a is neglected such that $Y_a = \text{j}1.1\,\text{mS}$ is purely imaginary. At this point Z_{in} is nearly infinite and the output impedance of the matching network Z_{out} is equal to preamplifier noise impedance $Z_{n,\text{opt}}$.

Second, $G_a = 0.14$ mS is included in simulations to evaluate its influence on Z_{in}. The matching network input impedance becomes $Z_{\text{in}} = 6.1 - \text{j}11.7\,\Omega$. Presented to the coil terminals, this impedance translates to a finite decoupling level of 35.2 dB. As anticipated, the output impedance of the matching network Z_{out} does not change, therefore, the noise figure is at the minimum noise figure of the preamplifier.

As a next step, all the ideal circuit components are replaced with models of off-the-shelf commercially available components to evaluate the influence of parasitic loss and component values deviation from initially calculated values. SMD inductor from Coilcraft Inc., Cary, Illinois, is used in this example. Because no 2 μH inductor is available off-the-shelf, the closest available value of 1.8 μH (1812 form factor with ceramic core) is used. To compensate for possible mismatch because of this new inductor value, the values of the capacitors were slightly adjusted. Because the capacitors have higher Qs, they can be either tunable or a combination of fixed value capacitors. Finally, the values are $C_1 = 433\,\text{pF}$, $L_2 = 1.8\,\mu\text{H}$, $C_3 = 8.4\,\text{pF}$, with corresponding quality factors $Q_1 = 1.0\times10^3$, $Q_2 = 68$, $Q_3 = 1.0\times10^4$. These new implemented values result in new $Z_{\text{in}} = 4.7 - \text{j}9.7\,\Omega$ and $Z_{\text{out}} = 154 - \text{j}110\,\Omega$. This Z_{in} is presented to the terminals of the coil, which translates to 27.1 dB of decoupling. The total simulated noise figure is 0.71 dB. The minimum noise figure extracted from the CAD model of the preamplifier is 0.14 dB. The excessive noise comes mainly from parasitic resistive loss in the matching network.

Finally, the circuit is built to verify maximum decoupling and minimum noise level experimentally. To measure the decoupling level, a reference matching network that emulates standard power matching is built. The difference between power matching and noise matching is taken as a measure of decoupling.[7] The reference circuit power matches the coil to a resistor by two capacitors, as shown in Figure 2.

The preamplifier, the fabricated Π-network, and the reference circuit are integrated on the same printed circuit board (PCB) to evaluate the decoupling. The coil can be connected to either the preamplifier or the reference matching network, as shown in Figure 2. The capacitors are realized as a parallel combination of fixed-value and variable capacitors to compensate for parasitics in the layout and component variations because of the fabrication tolerance. The inductor is 1.8 μH, and the measured total capacitances after fine-tuning

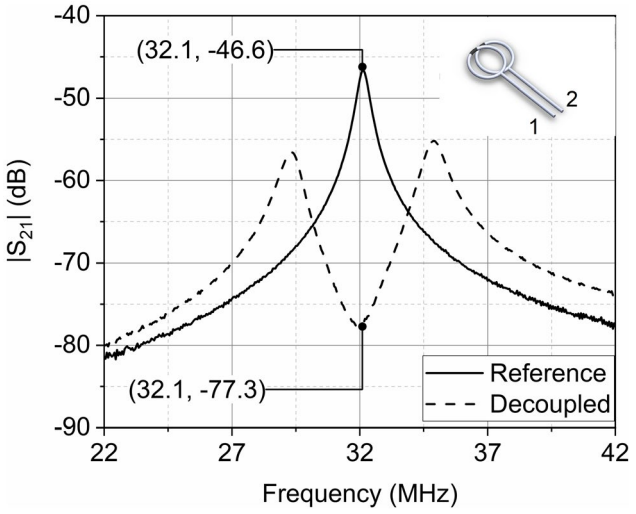

FIGURE 3 $|S_{21}|$ curves of the reference matching network and decoupling matching network. S_{21} is the transmission coefficient between the two terminals of a double probe pair. The difference between the two $|S_{21}|$ curves is taken as decoupling. The maximum decoupling is at the minimum of $|S_{21}|$ curve

are $C_1 = 326$ pF, $C_3 = 6.1$ pF, not far from the calculated values. A pair of overlapped probes (with coupling less than −80 dB) connected to a vector network analyzer (VNA), as shown in Figure 3, is used for decoupling measurements. The $|S_{21}|$ curves of the probe pair are recorded by VNA. The difference is taken as the measure of decoupling level.[7] The results are shown in Figure 3. The minimum of $|S_{21}|$ appears at the design frequency, indicating the maximum decoupling. The decoupling is 30.7 dB. This measured decoupling level is somewhat higher than the simulated value (27.1 dB). This may be attributed to small difference between element values in simulation and experiment setups, particularly the difference brought by variable capacitors and fabrication tolerances. The sample load of a coil may be subject to small change, resulting in a lower equivalent coil resistance, therefore, improving the decoupling.

To verify the optimal noise matching of the preamplifier, its output noise spectrum is observed. A minimum in the power spectral density should appear at the frequency where the impedance of the coil is transformed to the optimal noise impedance of the preamplifier. The entire circuit including preamplifier and coil is enclosed in a shielded box to suppress interference from man-made noise.[11] The output of the preamplifier is connected to a spectrum analyzer with the noise bandwidth set to 10 kHz. The recorded noise spectrum is shown in Figure 4 together with the simulation results. The measured noise spectrum exhibits a local minimum close to the design frequency, indicating that impedance at the input terminals of the preamplifier is close to the optimal noise matching condition (C2).

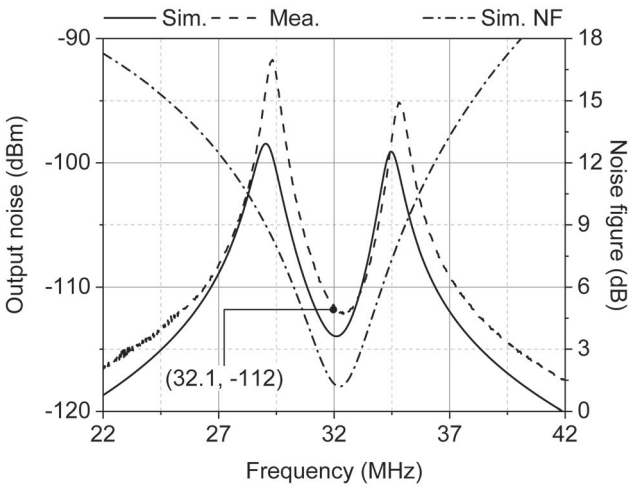

FIGURE 4 Verification of optimal noise matching. The simulated and measured noise spectra at the output terminals of the preamplifier in Figure 2. The measured noise spectrum exhibits a local minimum close to the design frequency 32.1 MHz, indicating that the impedance at the preamplifier input is close to the optimal noise matching condition. The simulated noise figure is plotted on the right vertical axis. The agreement between the simulated and measured circuit responses demonstrates the usefulness of Equations 2 and 4 for designing the matching network

To evaluate the described design approach in a wider range of frequencies, circuits for 64, 128, and 298 MHz are also developed as an example here. The anticipated imaging coil is 100 mm in diameter. It is loaded by a phantom and matched to the same preamplifier. At 298 MHz, the coil is segmented by three capacitors. The coil impedance Z_c, the input impedance of the preamplifer Z_{in}, and the optimal noise input impedance $Z_{n,\text{opt}}$, are obtained from the CAD model. As before, the Equations 2 and 4 are used to calculate the corresponding element values. The input parameters as well as the corresponding results of the design are listed in Table 1.

4 | DISCUSSION

It should be emphasized that even though only one out of four solutions is realized as an example here, any design provided by Equations 2 and 4 could be used. Ideally, all four circuits supposed to provide the same level of decoupling and optimal preamplifier noise matching. In practice, however, one solution can be more preferable than another. Below, several practical aspects of choosing a solution for actual realization are illustrated.

TABLE 1 T- and Π-network examples at 64, 128, and 298 MHz

f	64 MHZ	128 MHz	298 MHz
Z_c	0.97 + j105	5.0 + j224	3.7 + j60.5
Z_{in}	24.4 − j320	23.9 − j154	16.8 − j73.9
$Z_{n,\text{ opt}}$	114 + j42.5	86.9 + j63.2	33.1 + j61.2
T_1			
M_1	19.1 pF	5.0 pF	7.5 pF
M_2	68.7 nH	37.3 nH	6.4 nH
M_3	727 nH	154 nH	33.1 nH
T_2			
M_1	33.2 pF	6.6 pF	11.3 pF
M_2	90.0 pF	41.5 pF	44.9 pF
M_3	864 nH	229 nH	45.8 nH
Π_1			
M_1	21.6 pF	4.5 pF	7.4 pF
M_2	2.0 pF	1.1 pF	1.4 pF
M_3	644 nH	177 nH	202 nH
Π_2			
M_1	25.7 pF	6.61 pF	10.2 pF
M_2	3.0 μH	1.4 μH	35.3 nH
M_3	1.1 μH	234 nH	54.3 nH

Note: The units of Z_c, Z_{in} and $Z_{n,\text{ opt}}$ are all Ω. M_n (n = 1, 2, 3) correspond to either jX_n in T-networks or jB_n in Π-networks.

- One practical aspect is the sensitivity of the circuit to variation in element values. Depending on input parameters (impedance of the coil, input and optimal noise impedances of the preamplifier), one solution can be more sensitive than others. A standard approach is performing Monte Carlo analysis for each solution. A simpler approach is looking at the bandwidth of circuits which can indicate how sensitive the circuit is to the component values.[12] Out of four available solutions, it is more practical to choose those with wider bandwidths. Two examples of bandwidth analysis are given in Supporting Information.
- Another important aspect is the feasibility of the practical circuit realization. The designer should be aware of how close the calculated element values are to the limit of what is available off the shelf. Depending on the set of input parameters, some solutions of Equations 2 and 4 may give too low or too high component values. For example, the 1.4 pF capacitor at 298 MHz in Table 1 may be on the low side. Even though this low capacitance is available from the vendors, the final circuit might require extra care during PCB design and layout. In such circumstances, other solutions that require more reasonable component values are preferable.
- There are also cases where solutions with extreme value components can still be useful and even preferred. For example, if the components can be neglected because of extreme impedance value. A very large impedance component in parallel or a very small impedance component in series can sometimes be neglected without sacrificing the overall circuit performance. Then, the three-element network degenerates into two-element network, leading to even more compact and lower loss designs. In such cases, the solution with extreme component values can be preferred for practical realization.
- The last aspect is the flexibility of circuit with regard to co-integration with active switching components (diodes) that turn off the reception during the transmit pulse in an MRI system. For example, in T-network having one active switching component is sufficient to break the coil circuit and prevent the current flow. The Π-network needs two active switches (one series and one parallel) if a conventional switch driver of the scanner is used. In circumstances where compact design is a priority, the T-network with a single active switch may be preferred over the Π-network solution.

Finally, further analyzing Equations 1 and 3, it can be easily discovered that, if a short circuit is desired at the coil terminals rather than an open circuit, the design equations still apply, if one swaps $X \leftrightarrow B$, and $R \leftrightarrow G$. This implies that the solutions (2) and (4) are still applicable to the short-circuit case. This is particularly useful in self-resonant high impedance coils (HIC), which has gained a lot of attention recently.

5 | CONCLUSION

The design approach for the T-network and the Π-network is proposed to simultaneously provide high decoupling and optimal preamplifier noise matching. Design equations are derived according to requirements for decoupling and minimum preamplifier noise. Several design examples have been developed. One design example is fabricated and measured to demonstrate the design approach.

The approach offers four circuit solutions for a given coil and preamplifier combination. The general approach enables the use of arbitrary optimal noise impedance preamplifiers, at the same time minimizing the number of circuit components. It can be used in traditional low impedance as well as novel HIC.

ACKNOWLEDGEMENTS

This work was supported in part by the Danish National Research Foundation (DNRF 124).

ORCID

Wenjun Wang https://orcid.org/0000-0001-7781-9856
Vitaliy Zhurbenko https://orcid.org/0000-0002-1515-733X
Juan Diego Sánchez-Heredia https://orcid.org/0000-0002-8201-4136
Jan Henrik Ardenkjær-Larsen https://orcid.org/0000-0001-6167-6926

REFERENCES

1. Findeklee C. Array noise matching—generalization, proof and analogy to power matching. *IEEE Trans Antennas Propag*. 2011;59:452-459.
2. Roemer PB, Edelstein WA, Hayes CE, Souza SP, Mueller OM. The NMR phased array. *Magn Reson Med*. 1990;16:192-225.
3. Edelstein WA, Hardy CJ, Mueller OM. Electronic decoupling of surface-coil receivers for NMR imaging and spectroscopy. *J Magn Reson*. 1986;67:156-161.
4. Hyde JS, Rilling RJ, Jesmanowicz A. Passive decoupling of surface coils by pole insertion. *J Magn Reson*. 1990;89:485-495.
5. Reykowski A. Receiver systems. *Educ Sess ISMRM*. 2006.
6. Johansen DH, Sanchez-Heredia JD, Zhurbenko V, Ardenkjær-Larsen JH. Association and dissociation of optimal noise and input impedance for low-noise amplifiers. *IEEE Trans Microw Theory Tech*. 2018;66:5290-5299.
7. Reykowski A, Wright SM, Porter JR. Design of matching networks for low noise preamplifiers. *Magn Reson Med*. 1995;33:848-852.
8. Vidkjær J. Chapter II, RF-circuits. In: *Class Notes, 31415 RF-Communication Circuits*. http://rftoolbox.dtu.dk/book/Ch2.pdf.
9. Sanchez-Heredia JD, Baron R. Szocska Hansen ES, Laustsen C, Zhurbenko V, Ardenkjar-Larsen JH. Autonomous cryogenic RF receive coil for 13C Imaging of Rodents at 3 T. *Magn Reson Med*. 2019;84 1-12.
10. ElCry1-u datasheet. http://elcry.com/.
11. Vidkjær J. Chapter IV, Noise and distortion. In: *Class Notes, 31415 RF-Communication Circuits*. http://rftoolbox.dtu.dk/book/Ch4.pdf.

12. Vinther JMO, Zhurbenko V, Albannay MM, Ardenkjær-Larsen JH. Design of a local quasi-distributed tuning and matching circuit for dissolution DNP cross polarization. *Solid State Nucl Magn Reson*. 2019;102:12-20.

SUPPORTING INFORMATION

Additional Supporting Information may be found online in the Supporting Information section.

FIGURE S1 Reduced circuits

FIGURE S2 Bandwidths of circuits in Figure 1 as a function of Q for the 32.1 MHz case. Higher coil Q entails narrower bandwidth. In this case, the T_1 network is the most narrowband

FIGURE S3 Bandwidths of circuits in Figure 1 as a function of Q for the 128.1 MHz case. In this case, the four networks have similar bandwidths

How to cite this article: Wang W, Zhurbenko V, Sánchez-Heredia JD, Ardenkjær-Larsen JH. Three-element matching networks for receive-only MRI coil decoupling. *Magn Reson Med*. 2020;00:1–7. https://doi.org/10.1002/mrm.28416